Supplementary Information

Tumor-initiating stem-like cells in human prostate cancer exhibit increased NF-kB signalling

Vinagolu K. Rajasekhar[1, 4], Lorenz Studer[1], William Gerald[2], Nicholas D. Socci[3], and Howard I. Scher[4]

[1]Stem Cell Center and Developmental Biology Program, Sloan-Kettering Institute, [2]Pathology, [3]Computational Biology Center, [4]Genitourinary Oncology Service, Department of Medicine, Memorial Sloan-Kettering Cancer Center, New York, NY 10065, USA

Supplementary Figures

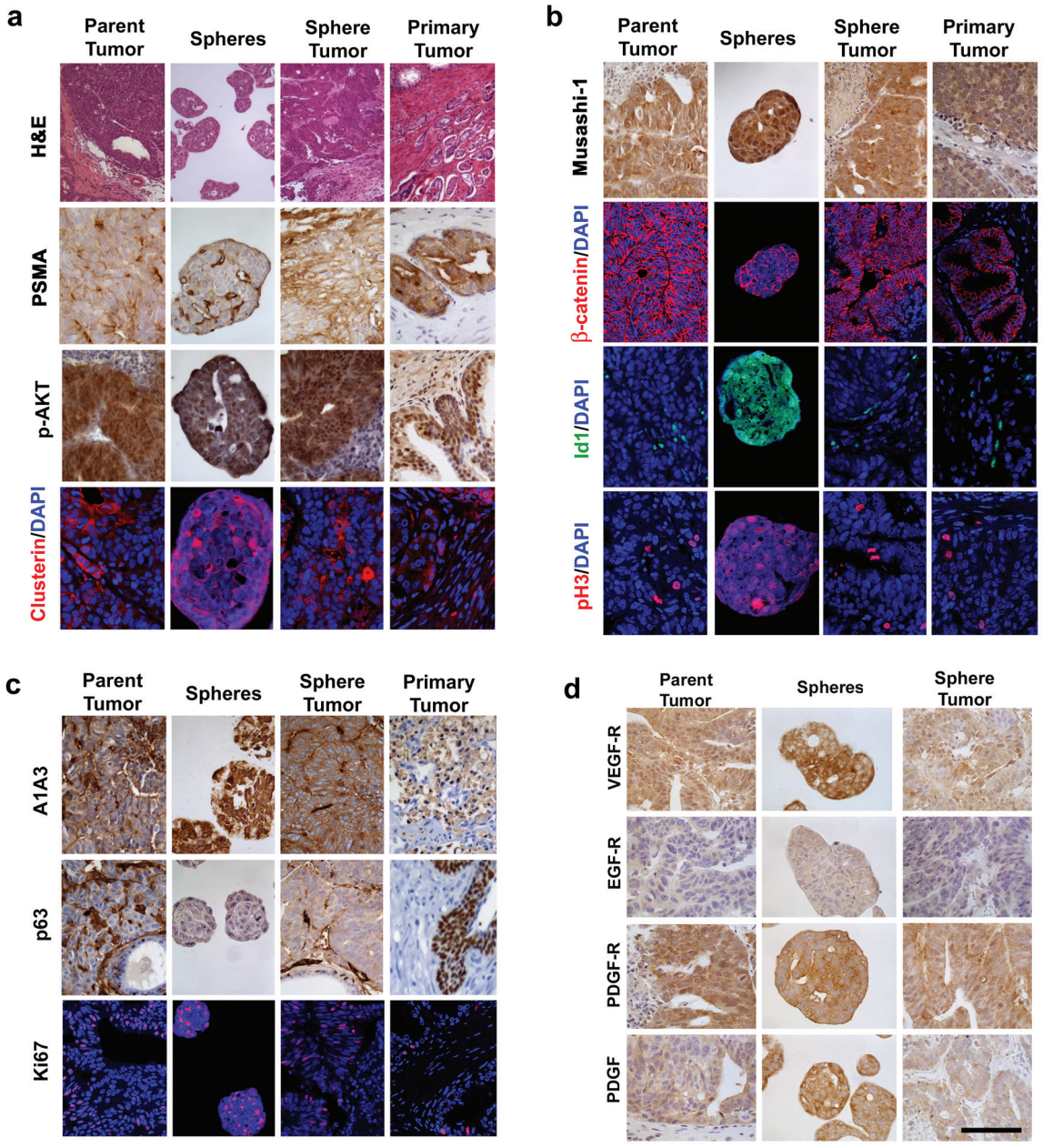

Supplementary Figure S1: Comparative histopathology and immunochemistry of stem-like sphere-forming cells and tumors. Primary sphere cells are compared to the human prostate CWR22 OT-tumor (parent tumor), primary sphere-derived tumors (sphere tumor) and human patient primary tumor (primary tumor). Immunohistochemistry (IHC) or immunofluorescence (IF) was utilized. DAPI in IF marks nuclear staining. (a) Tumor histology is characterized by hematoxylin and eosin (H&E) stain. Prostate cell identity (PSMA by IHC), and oncogenic signaling (p-AKT by IHC, and Clusterin/DAPI by IF) were assessed. (b) Relative expression of putative stem cell markers (Mushashi-1 by IHC; β-catenin, and ID1 by IF), and cell proliferation marker (Phospho-Histone 3[pH3] by IF) were studied. (c) Relative to the tumor sets in comparison, primary spheres were stained for decreased expression of basal cell marker, p63 (IHC); increased expression of the proliferating cell marker, Ki67 (IF); and similar levels of epithelial cell marker, the pan-cytokeratins A1A3 (IHC), and associated clusterin (IF). (d) Similar staining patterns were observed in all the sets for oncogenic growth receptors such as VEGF-R, EGF-R, and PDGF-R as well as for growth factor receptor ligands such as PDGF by IHC. Scale bar = 50μm.

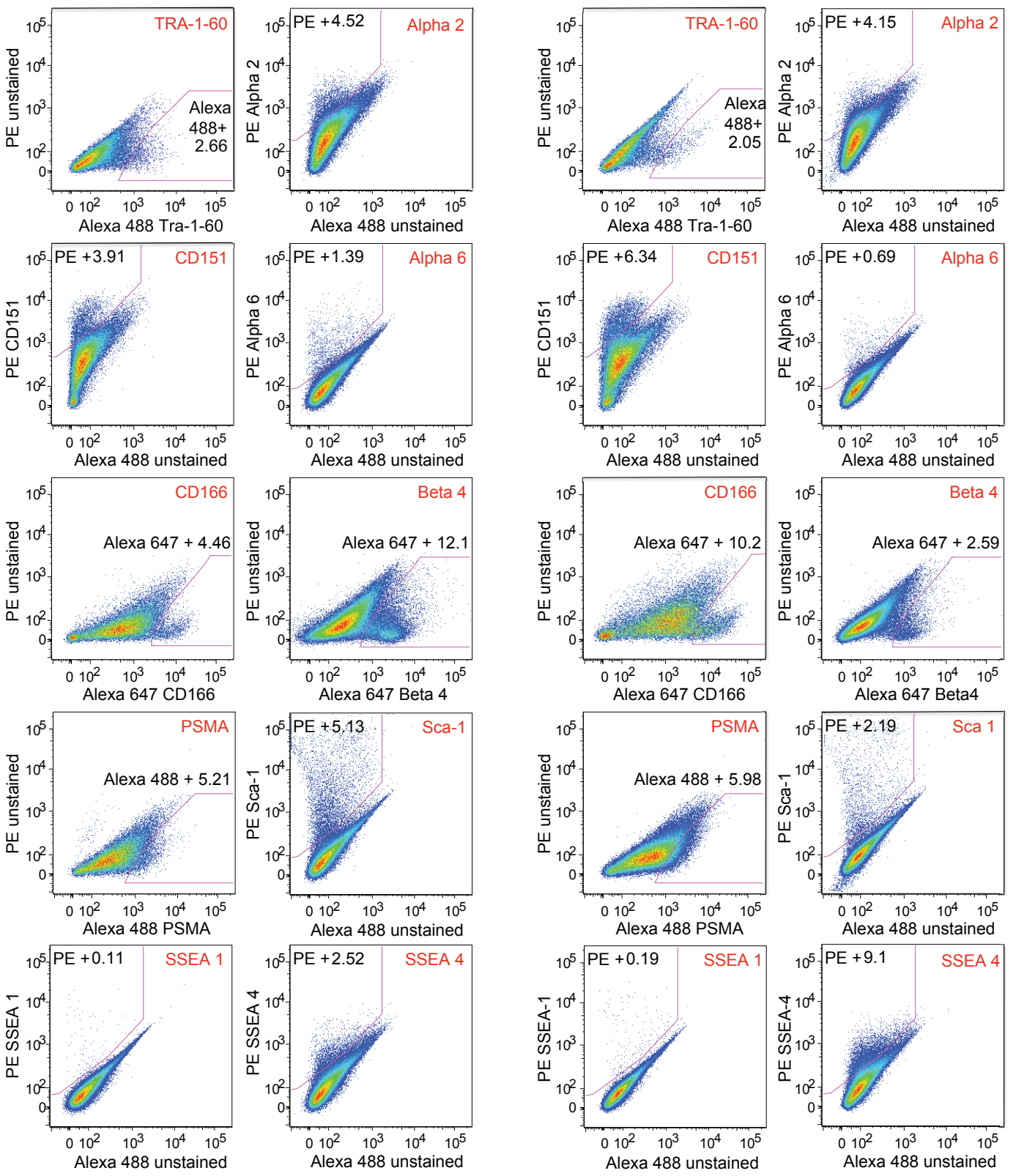

Supplementary Figure S2: Isolation of various marker-positive cells in human prostate tumor. The same number ($2x10^6$) of cells from the CWR22 OT-tumor was simultaneously transplanted at SC locations in NOD/SCID mice and nude mice. At 4 weeks following the transplantation, tumor cells were analyzed by FACS for marker expression. Singlet gated unstained cells were used to draw gates to identify Alexa 488+, Alexa 647+, APC+, FITC+, or PE+ -conjugated antibody-reactive cell populations. Identities of fluorochromes conjugated to antibodies are denoted in each plot. Value at each of the above gates identifies frequency of its parent gate. The frequency of fluorochrome positivity measuring the percentage of marker-expressing cells is shown.

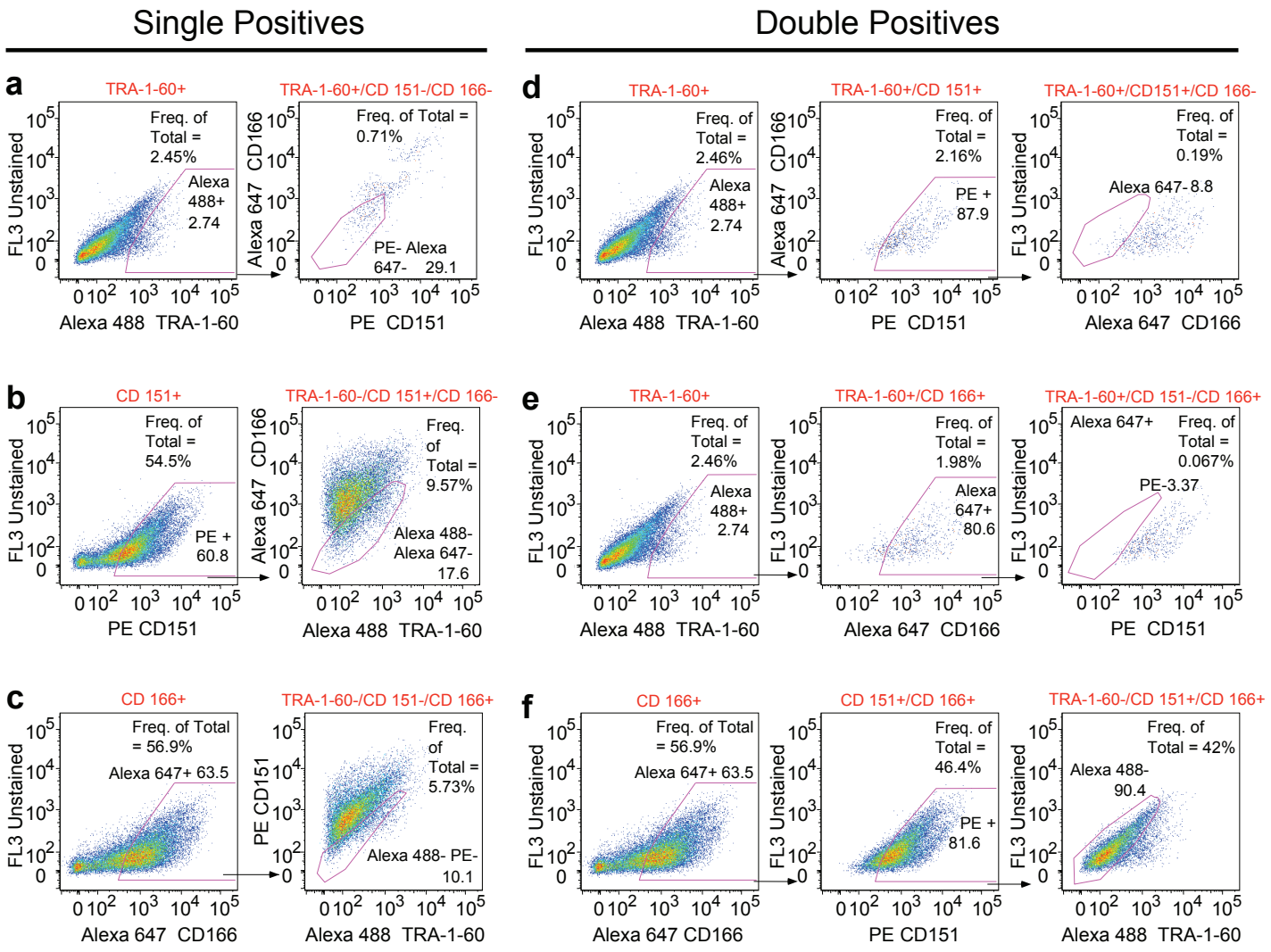

Supplementary Figure S3: Strategy for isolation of single-/double- marker-positive cells in human prostate tumor. The CWR22-OT tumor cells were analyzed by FACS for marker expression. **Single Positives:** Cells expressing only one of the above three markers (single positives) were gated from the total tumor cells by excluding cells that express the other two markers as denoted. (a) Alexa 488 conjugated, anti-TRA-1-60-positive cells were gated to exclude cells positive for PE conjugated anti-CD151 and Alexa 647 conjugated anti-CD166. (b) PE conjugated anti-CD151 positive cells were gated to exclude cells positive for Alexa 488 conjugated anti-TRA-1-60 and Alexa 647 conjugated anti-CD166. (c) Alexa 647 conjugated anti-CD166 positive cells were gated to exclude cells positive for Alexa 488 conjugated anti-TRA-1-60 and PE conjugated anti-CD151. **Double Positives:** Cells expressing only two of the three markers (double positives) were gated from the total tumor cells by excluding cells expressing the third one. (d) Alexa 488 conjugated anti-TRA-1-60-positive cells were gated to include only those that are also positive for PE conjugated anti-CD151, and to exclude cells positive for Alexa 647 conjugated anti-CD166. (e) Alexa 488 conjugated anti-TRA-1-60-positive cells were gated to include only those that are also positive for Alexa 647 conjugated anti-CD166, and to exclude any cells positive for PE conjugated anti-CD151. (f) Alexa 647 conjugated anti-CD166 positive cells were gated to include only those that are also positive for PE conjugated anti-CD151, and to exclude cells that are also positive for Alexa 488 conjugated anti-TRA-1-60. Value at each of the above gates identifies frequency of its parent gate. Frequency of total at the top of each FACS plot represents the percent frequency out of total tumor cells. The frequency of fluorochrome positivity measuring the percentage of marker-expressing cells is shown.

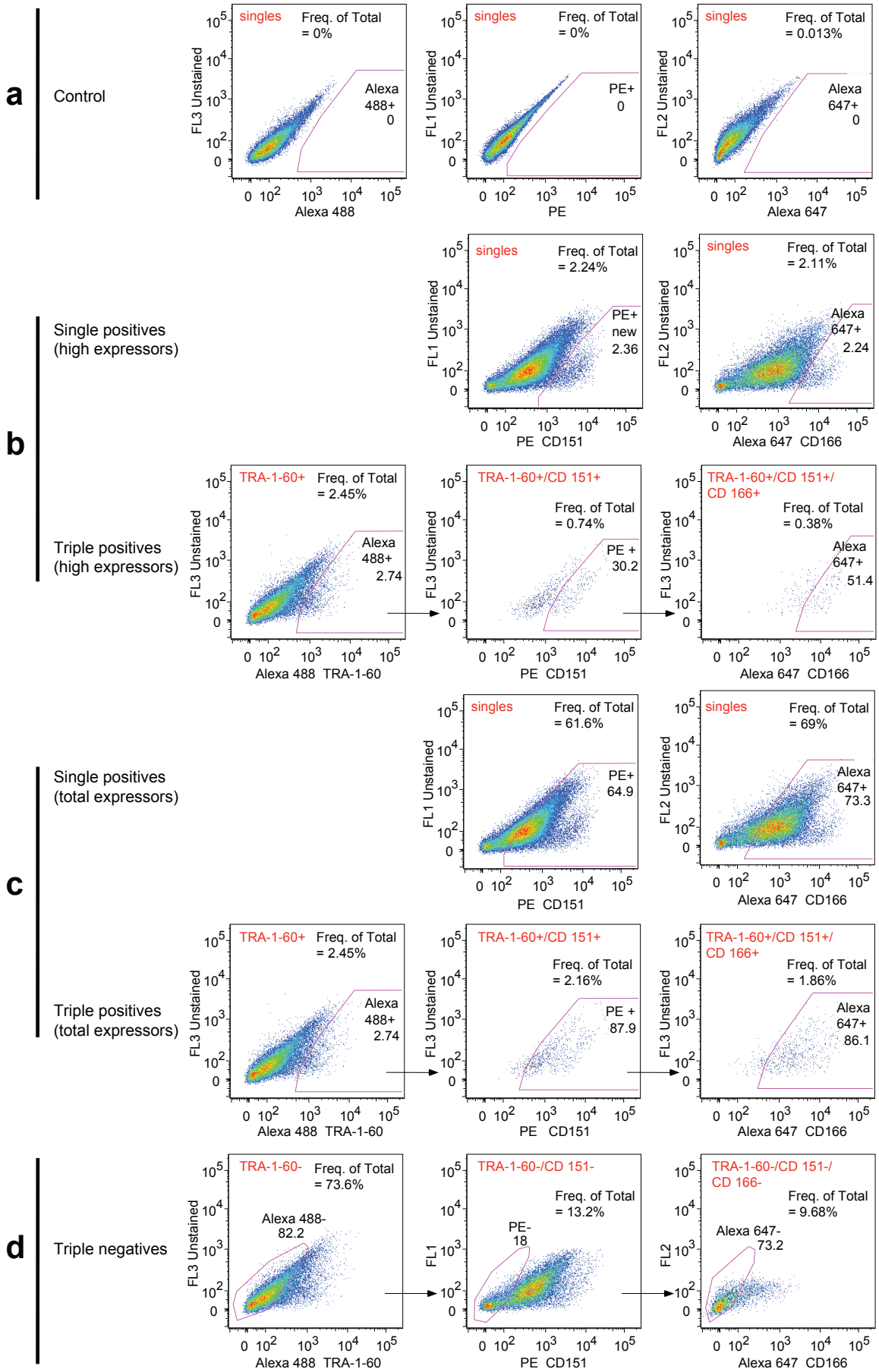

Supplementary Figure S4: Strategy for isolation of triple-marker-positive cells in human prostate tumor. The CWR22-OT tumor cells were analyzed by FACS. (a) Alexa 488 conjugated anti-TRA-1-60-positive cells from the tumor were first gated to include those cells that are also positive for PE conjugated anti-CD151, and finally gated to select only those that are in turn positive for Alexa 647 conjugated anti-CD166. The total tumor cells positive for all the above three markers (triple positives) were gated to include only brightly positive cells (high expressors) (b) or to include all those that are grossly positive (total positives)(c). Corresponding single positives are shown for comparison within the same gates. Unstained tumor cells served as control to demonstrate no interference of autofluorescent cells within the above gates (a). Cells that do not express all these three markers (triple negatives) were gated with the similar strategy, but by sequentially gating for the cells that were negative for expression of all the above three markers (d). Value at each of the above gates identifies frequency of its parent gate. Frequency of total at the top of each FACS plot and the percentage of marker expressing cells shown are as described in Supplementary Figure S3.

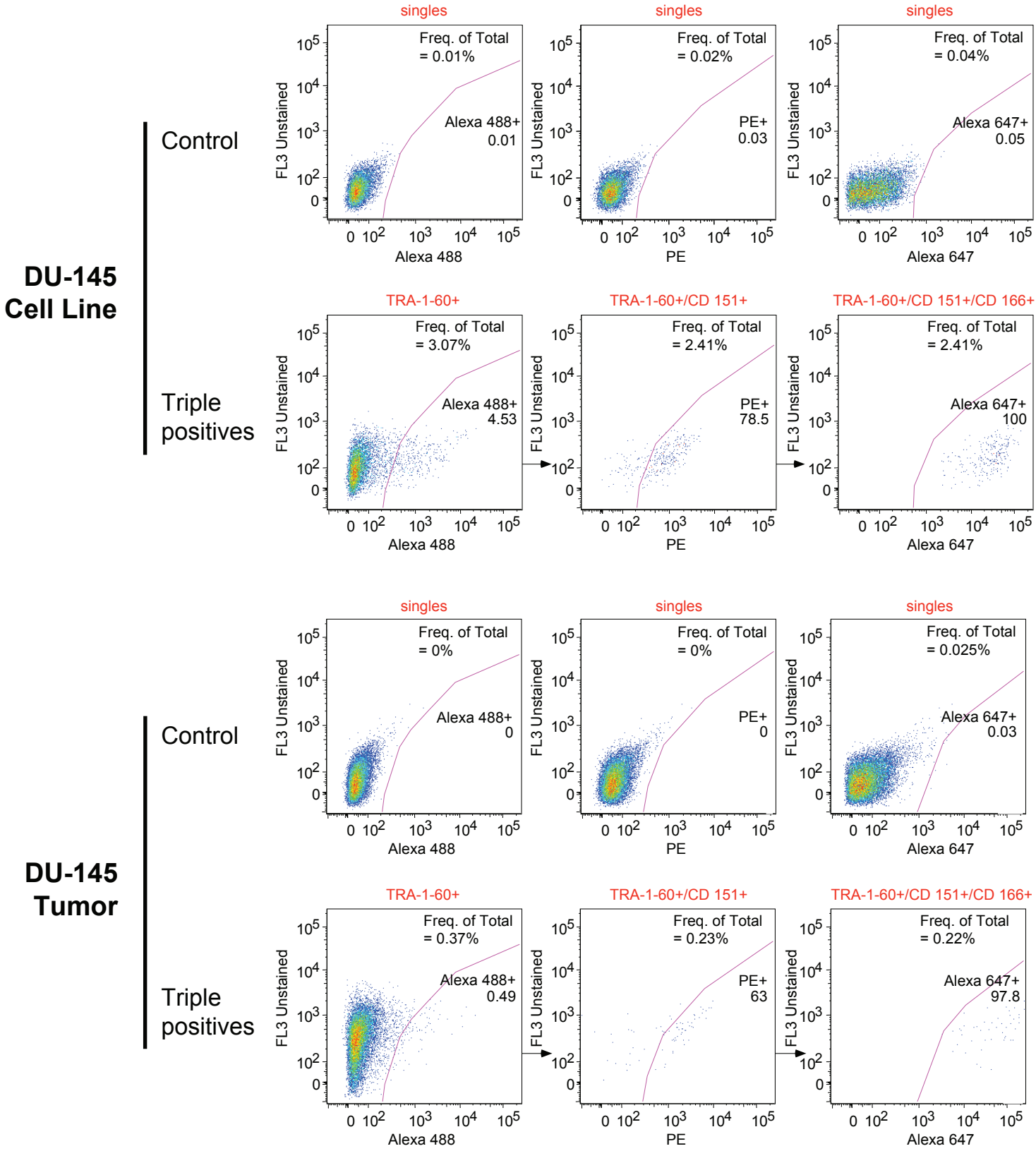

Supplementary Figure S5: Strategy for isolation of triple-marker-positive cells in DU-145 tumors. The tumor cell lines and the cell line-derived tumor cells were analyzed by FACS for marker expression. Alexa 488 conjugated anti-TRA-1-60-positive cells were gated to include only those cells that are also positive for PE conjugated anti-CD151, and finally gated to select only those that are in turn positive for Alexa 647 conjugated anti-CD166. Unstained tumor cells served as control to demonstrate that there was no considerable interference of autofluorescent cells within the above gates. Triple negative cells were gated with a similar strategy, but by sequentially gating the cells that were negative for expression of all the above three markers. Value at each of the above gates identifies frequency of its parent gate. Frequency of total at the top of each FACS plot represents the percent frequency out of total tumor cells. The frequency of fluorochrome positivity measuring the percentage of marker-expressing cells is shown.

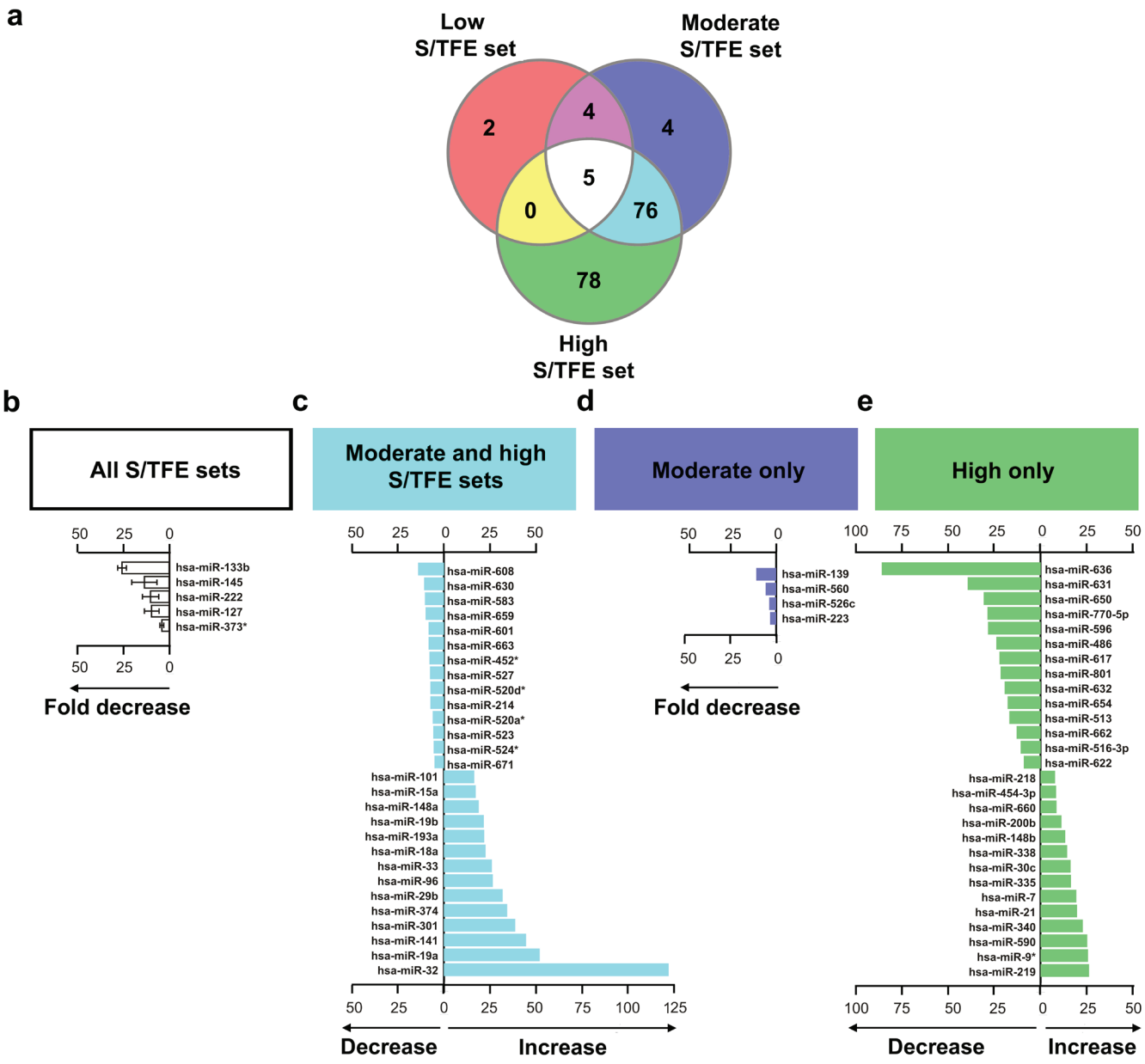

Supplementary Figure S6: Global miRNA expression in marker-positive human prostate TICs. a) Venn-diagram of genes differentially expressed in prospectively purified CWR22–OT-tumor cells with low (cells grossly expressing EpCAM, CD44, or α2- integrin), moderate (cells grossly expressing TRA-1-60, CD151, or CD166) or high (triple marker-positive cells) sphere/tumor forming efficiencies (S/TFE). Gene expression data in no sphere-forming cells (β4-integrin-positive cells) and the total tumor cells were used as base line expression controls. (b-e) Catalogue of top differentially expressed genes: b- shared among all the above three data sets, c- shared between moderate and high S/TFE data sets, d- expressed specifically in moderate S/TFE data set, and e- expressed specifically in high S/TFE data set.

Supplementary Table

Supplementary Table S1: Antibody Resource

Antibody Identity	Catalogue# / Clone	Source
14-3-3σ (1.N.6)	ab14123	Abcam
4E-BP1 (phospho-Ser 65)	clone 174A9	Cell Signaling Technology
AKT (phospho-Ser473)	clone 193H12 for WB	Cell Signaling Technology
AKT total	9272	Cell Signaling Technology
Alpha B Crystallin	ab13497	Abcam
AR (Androgen receptor)	clone F39.4.1 for IHC	Biogenex
AR (Androgen receptor)	clone AR441 for WB	DAKO
Carbonic anhydrase	clone H-120	Santa Cruz Biotechnology
CD133/1-APC	clone AC133C3	Miltenyi Biotec
CD133/2-APC	clone 293C3	Miltenyi Biotec
CD151/APC/PE	clone 21012	R&D Systems
CD166(ALCAM)/APC/PE	clone 105901	R&D Systems
CD44-APC/PE	G44-26	BD BioSci/Phar
CD49b (α2-Integrin)-PE	clone 12F1-H6	BD BioSci/Phar
CD49f(α6-Integrin)-PE	clone GoH3	BD BioSci/Phar
Cleaved caspase	9661	Cell Signaling Technology
Clusterin	clone CLI-9	Santa Cruz Biotechnology
Cytokeratin 18 (CK18)	ab52948	Abcam
Cytokeratin 5 (CK5)	D5/16 B4	Covance
Cytokeratin 8 (CK8)	ab9023	Abcam
Cytokeratins (Pan) A1/A3	clone A1 and A3	Biogenex
Desmin	clone D33	DAKO
E-cadherin	clone 36/E-Cadherin	BD BioSci/Phar
E-cadherin (ECH-4)	ECH-4	Ventana
EGFR	clone 31G7	Zymed
eIF-4E (phospho-Ser209)	9741	Cell Signaling Technology
EpCAM-APC/PE/FITC	clone EBA-1	BD BioSci/Phar
ERK (phospho-44/42 MAP Kinase)	clone 20G11	Cell Signaling Technology
GAPDH	clone 7B	Santa Cruz Biotechnology
H-2K^{d} –FITC	clone SF1-1.1	BD BioSci/Phar
Histone H3 (phospho-Ser 31)	07-679	Upstate Biotechnology
HLA-ABC-PE	clone G46-2.6	BD BioSci/Phar
ID1	clone BCH-1/195-14	Biocheck
IGFBP7	ab51392	Abcam
IGF-I Receptor β	clone 111A9	Cell Signaling Technology
IL6	clone H183	Santa Cruz Biotechnology
Ki67	clone MIB-1	DAKO

Maspin	clone NCL-Maspin	Nova Castra
MCL1	8C6D4B1	Abcam
MET receptor	clone C-28	Santa Cruz Biotechnology
Musashi-1	clone 282613	R&D Systems
NFkB p65	ab16502	Abcam
NFkB p65-K310 acetylated	ab19870	Abcam
NFKBIA	clone E130	Abcam
Nkx3.1	AB5983	Chemicon/Millipore
p63	clone 4A4	DAKO
PARP	clone 51-6639GR	BD BioSci/Phar
PDGF-a	clone N-30	Santa Cruz Biotechnology
PDGFR-a	clone SC-338	Santa Cruz Biotechnology
PKC (pan-βII; phospho-Ser660)	9371	Cell Signaling Technology
PKCα	2056	Cell Signaling Technology
PKCα (phospho-Thr497)	clone EP2608Y	Epitomics
PKCα (phospho-Thr638/641)	9375	Cell Signaling Technology
PKCζ/λ (phospho-Thr410/403)	9378	Cell Signaling Technology
PKD/PKCμ (phospho-Ser744/748)	2054	Cell Signaling Technology
PSA (Prostate specific antigen)	ERPr8	Biogenex
PSMA(Prostate specific membrane antigen)	clone 7C12	Epitomics
Racemase	clone P504S	Zeta
S6RP (phospho-Ser 235/236)	clone 2F9	Cell Signaling Technology
S6RP (S6 Ribosomal protein)	2217	Cell Signaling Technology
Sca1-PE	50589	BD BioSci/Phar
Sox9	AB5535	Chemicon/Millipore
SSEA1-PE	clone MC-480	Chemicon/Millipore
SSEA4-PE	clone ebioMC-813-170	eBioScience
TRA-1-60	clone TRA-1-60 for WB	Cell Signaling Technology
TRA-1-60	clone TRA-1-60 for FACS	Chemicon/Millipore
TRA-1-81	clone TRA-1-81	Chemicon/Millipore
VEGF-R2	clone C-1158	Santa Cruz Biotechnology
ZO1	33-9100 for IHC	Zymed
ZO-1	ab41893 for WB	Abcam
β4-integrin	clone 3E1	MSKCC Monoclonal facility
β-catenin	clone C2206	Sigma

Supplementary Methods

Animal and human prostate tumor-xenografts. Two independent human primary prostate tumors, maintained as mouse OT xenografts, were used for our studies. Dr. Thomas G. Pretlow[25] of Case Western Medical Center, Cleveland, OH, provided us with orthotopically transplantable human prostate CWR22 tumors maintained as xenografts in athymic nude (nu/nu) male mice. Routine maintenance of the CWR22 tumor, which involves preparation, processing, transplantation, and functional evaluation of the transplant, has been described previously and was performed strictly according to the approved protocols[25, 58, 59]. Prior (at least 2-3 days) to tumor transplantation, the mice were supplemented with 5-α-dihydroxy testosterone (DHT; 12.5 mg pellet - 90-day release; Innovative Research of America, Sarasota, FL) as a subcutaneous implant. An additional human prostate tumor (PC-82)[60, 61] was originally obtained as a xenograft-tumor grown in non-obese diabetes/severe combined immuno-nonobese (NOD/SCID) mice from Dr. John Isaacs (Johns Hopkins University) and subsequently maintained in NOD/SCID-mice lacking the interleukin-2 gamma receptor. OT and SC transplantations (after mixing with Matrigel, a matrix basement membrane [BD Biosciences]) into each flank of the mice were performed according to animal care and use protocols approved by the Research Animal Resource Center at Memorial Sloan-Kettering Cancer Center (MSKCC), New York, NY. Tumor growth was evaluated regularly (every 3-4 days) by palpation, and size of the SC tumor was measured by calipers. Tumors were located at the injection sites, and no SC metastases were observed. Whenever size of tumors caused distress to the mouse, surgical removal of the tumor was opted for to facilitate the continuous monitoring of the other injection sites. Requirement of testosterone for tumor growth was routinely confirmed for both OT and SC locations. Tumors were harvested for cellular and biochemical analysis at four weeks after transplantation unless otherwise stated.

Cell cultures. The human normal prostate epithelial cells, the PrEC and the RWPE1, were obtained from Lonza and American Type Culture Collection (ATCC) respectively, and the cell lines were maintained according to the supplier's instructions. The tumorigenic human prostate metastatic cancer cell lines (bone metastasis-derived PC-3, vertebral metastasis-derived VCaP, and brain metastasis-derived DU-145), were all obtained from the ATCC and propagated as per the supplier's protocols.

Clinical tumor specimens. Harvesting of human prostate tumor specimens was performed in the institutional Tumor Procurement Service of the Pathology Core Facility in accordance with the approved IRB protocol as well as the MSKCC Human Biospecimen Utilization Committee. Prostate specimens from consenting patients were serially sectioned for gross examination. Biopsies of human patient tumor specimens and the patient-matched normal tissues were carried out using 6 mm dermal punches of the excised organs under the supervision of genitourinary pathologists. Similarly, additional human patient specimens were obtained from breast, ovary and colon tumors.

Antibodies. Antibody resource was compiled as per Supplementary Table S1. In cases where antibodies against the same epitope were obtained from multiple vendors, the specific source is listed in the text. All antibodies were employed at dilutions suggested by the manufacturers. For cell sorting, Allophycocyanin (APC), Phycoerythrin (PE), Fluorescein isothiocyanate (FITC), Alexa 488, Alexa 647, or Alexa 568 fluorochrome conjugated primary or appropriate secondary antibodies were used as indicated. TRA-1-60, CD151, CD166, human β4-integrin, and PSMA antibodies were conjugated by the MSKCC core facility using a commercially available kit (Invitrogen). For western blotting secondary antibodies conjugated with horse-radish peroxidase were used (Jackson Immunoresearch Laboratories). For immunofluorescence histochemistry analyses, appropriate secondary antibodies conjugated to specific fluorochromes were used (Vector Labs). Species-matched primary antibodies were also used as specificity controls where appropriate.

Light microscopy, histopathology, and immunostaining. Dissociated tumor and sphere cells were visualized under phase-contrast microscopy on an inverted microscope (Olympus IX71). Prostate tumors and primary spheres were fixed in 4% para-formaldehyde, paraffin embedded, sectioned at 4 μm thickness, and stained with hematoxylin and eosin (H&E) analysis for histopathology analyses. The paraffin sections were de-paraffinized in xylene, rehydrated with distilled water, blocked with 10% fetal calf serum for 30 minutes at room temperature, and then incubated with primary antibodies at the routinely titrated/optimized concentrations in our histology immuno-core facility. Fresh frozen tissues were embedded in optimal cutting temperature (OCT) compound (Tissue-Tek, Sakura), cryostat sectioned, fixed in ice cold acetone for 10 minutes on ice, and air-dried. Immunohistochemical analysis was performed following blocking for nonspecific binding and further processing with the primary antibodies. The immunohistochemical detection was performed with a Discovery XT system (Ventana Medical Systems) at the Molecular Cytology Core Facility at MSKCC, and also manually as described below. For immunofluorescence analysis, Alexa 568 detection was performed with Streptavidin-HRP D (Ventana Medical Systems), followed by incubation with Tyramide Alexa Fluor 568 (Invitrogen, TSA kit #4 HRP-goat antimouse IgG and Alexa Fluor 568 tyramide). Alexa 488 detection was performed with Streptavidin-HRP D (Ventana Medical Systems), followed by incubation with Tyramide-Alexa Fluor 488 (Invitrogen, TSA kit #12). Primary antibody binding was recognized either by immunohistochemistry involving the biotinylated secondary antibody (Vector) VECTASTAIN ABC peroxidase system and peroxidase substrate DAB kit (Vector), or by immunofluorescence involving the fluorochrome (Alexa 488 or Alexa 568) conjugated secondary antibodies or the biotinylated secondary antibodies detected by Streptavidin-Rhodamine (Red). The stained sections were mounted with permount, and in some cases counterstained with DAPI (5μg/ml) for 10 minutes at room temperature before mounting with fluorescence anti-fade medium (Mowiol, Calbiochem). Bright field and fluorescent images were acquired with Carl Zeiss Axiophot microscope using Axiovision software. Fluorescent images were also captured with the Leica SP2 AOBS confocal microscope.

Cell cycle analysis. Cell cycle analysis was carried out as previously described[62], with minor modifications. A minimum of 2 x 10^5 cells were pelleted, washed once in phosphate buffered saline, and washed twice with FACS analysis buffer containing propidium iodide (50 µg /ml; Sigma), sodium citrate (0.1%; Sigma), 0.1% Triton X-100, and RNase A (200 µg/ml) prepared in phosphate buffered saline. The final cell preparation was resuspended in FACS analysis buffer and incubated for 15 minutes in the dark, spun down, and kept on ice in the dark until further processing (cell cycle analysis was performed usually within a time span of 15 minutes). Cell samples were analyzed using a FACS Caliber flow cytometer (Becton Dickinson), and the cell cycle values were obtained by standard histogram analysis using MultiCycle software (Phoenix Flow Systems).

Supplementary References

58. Nagabhushan, M. et al. CWR22: the first human prostate cancer xenograft with strongly androgen-dependent and relapsed strains both in vivo and in soft agar. *Cancer Res* **56**, 3042-3046 (1996).
59. Sirotnak, F.M. et al. Microarray analysis of prostate cancer progression to reduced androgen dependence: studies in unique models contrasts early and late molecular events. *Mol Carcinog* **41**, 150-163 (2004).
60. Hoehn, W., Walther, R. & Hermanek, P. Human prostatic adenocarcinoma: comparative experimental treatment of the tumor line PC 82 in nude mice. *Prostate* **3**, 193-201 (1982).
61. Kyprianou, N., English, H.F. & Isaacs, J.T. Programmed cell death during regression of PC-82 human prostate cancer following androgen ablation. *Cancer Res* **50**, 3748-3753 (1990).
62. Desbordes, S.C. et al. High-throughput screening assay for the identification of compounds regulating self-renewal and differentiation in human embryonic stem cells. *Cell Stem Cell* **2**, 602-612 (2008).